OCS Study
MMS 2006-051

Biodegradation in the Subsurface as a Selective Filter for Natural Petroleum Emissions

Final Technical Summary

Final Study Report

U.S. Department of the Interior
Minerals Management Service
Pacific OCS Region

OCS Study
MMS 2006-051

Biodegradation in the Subsurface as a Selective Filter for Natural Petroleum Emissions

Final Technical Summary

Final Study Report

Authors
George D. Wardlaw
Christopher M. Reddy
Robert K. Nelson
J. Samuel Arey
David L. Valentine

Principal Investigator
David L. Valentine

Prepared under MMS Cooperative Agreement No. 14-35-0001-31063
by
Coastal Marine Institute
Marine Science Institute
University of California
Santa Barbara, CA 93106-6150

U.S. Department of the Interior
Minerals Management Service
Pacific OCS Region

Camarillo
November 2006

Disclaimer

This report has been reviewed by the Pacific Outer Continental Shelf Region, Minerals Management Service, U.S. Department of the Interior and approved for publication. The opinions, findings, conclusions, or recommendations in this report are those of the authors, and do not necessarily reflect the views and policies of the Minerals Management Service. Mention of trade names or commercial products does not constitute an endorsement or recommendation for use. This report has not been edited for conformity with Minerals Management Service editorial standards.

Availability of Report

Extra copies of the report may be obtained from:

U.S. Dept. of the Interior
Minerals Management Service
Pacific OCS Region
770 Paseo Camarillo
Camarillo, CA 93010
Phone: 805-389-7621

A PDF file of this report is available at:
http://www.coastalresearchcenter.ucsb.edu/CMI/

Suggested Citation

The suggested citation for this report is:

Valentine, David L. Biodegradation in the Subsurface as a Selective Filter for Natural Petroleum Emissions. MMS OCS Study 2006-051. Coastal Research Center, Marine Science Institute, University of California, Santa Barbara, California. MMS Cooperative Agreement Number 14-35-0001-31063. 35 pages.

Table of Contents

FINAL TECHNICAL SUMMARY 1

FINAL STUDY REPORT 5

Abstract 6
Introduction 6
References Cited 13
Acknowledgements 16
Supplementary Methods 17
Appendix 1 21
Supplemental References 28

List of Tables

Table S1. Concentrations of major hydrocarbon classes 20

List of Figures

Figure 1. GCxGC with flame ionization detection (FID) chromatograms 8
Figure 2. Difference chromatograms 9
Figure 3. Cumulative rank-distribution for all hydrocarbons..... 10
Figure 4. Raw chromatograms transformed 11
Figure S1. An image of oil seeping from the sea floor 17
Figure S2. A graph of *n*-alkyl cyclopentanes and cyclohexanes 19

FINAL TECHNICAL SUMMARY

STUDY TITLE: Weathering of Aromatic Compounds in the Coastal Marine Environment: Quantifying Rates of Microbial Metabolism

REPORT TITLE: Biodegradation in the Subsurface as a Selective Filter for Natural Petroleum Emissions

CONTRACT NUMBER: 14-35-0001-31063

SPONSORING OCS REGION: Pacific

APPLICABLE PLANNING AREA(S): Southern California

FISCAL YEAR(S) OF PROJECT FUNDING: FY 02/03, FY 03/04, FY 04/05

COMPLETION DATE OF REPORT: November 2006

COSTS: FY 02-04 – $83,071

CUMULATIVE PROJECT COST: $83,071

PROJECT MANAGERS: Russell J. Schmitt

AFFILIATION: Coastal Research Center, Marine Science Institute, University of California, Santa Barbara, CA 93106

ADDRESS: University of California, Santa Barbara, CA 93106

PRINCIPAL INVESTIGATOR: David L. Valentine

ADDRESS: Department of Earth Science and Marine Science Institute, University of California, Santa Barbara, CA 93106

KEY WORDS: oil seep, weathering, aromatic hydrocarbons, biodegradation

BACKGROUND: Several tons of oil seep from the sea floor into the waters of coastal California each day. The oil is converted to tar by an ill-defined combination of chemical, biological and physical processes – collectively referred to as weathering. The broad focus of this project was to determine the microbial role in the weathering process – particularly as it relates to aromatic hydrocarbons.

OBJECTIVES: The objectives of this work were to investigate the nature of hydrocarbon weathering processes, particularly those mediated by microbes.

DESCRIPTION: Initially we planned to use a radiotracer approach to investigate the consumption of specific aromatic hydrocarbons. Soon after the project was initiated we became aware of a new analytical approach better suited to the investigation of microbial hydrocarbon weathering: two-dimensional comprehensive gas chromatography (GC×GC). At the same time, the instrument we planned to use for the radiotracer work was pulled from the market, confirming our decision to switch techniques.

Completed research focused on the detailed compositional changes that occur in petroleum from the time of formation, through subsurface migration, to the point of seepage from the seafloor and finally to spreading at the sea surface. This was achieved applying the new technique of comprehensive two-dimensional gas chromatography to a natural progression of petroleum samples collected from subsurface reservoirs, the sea floor and the sea surface.

STUDY RESULTS: Environmental studies designed to assess the patterns and rates of petroleum weathering during migration and seepage has been completed, the samples were analyzed using GC×GC, and a manuscript has been submitted for publication. This manuscript highlights the power of the approach developed in this study, and shows detailed chemical changes in over 4000 specific hydrocarbon compounds. Biodegradation is shown to be the dominant process in the subsurface, accounting for a loss about half the total petroleum hydrocarbon. Once petroleum reaches the sea floor, evaporative processes act rapidly, causing a loss of about 10% of the total petroleum hydrocarbon – on the order of minutes. Other physical-chemical processes, such as adsorption to a thin layer, also seem to drive compositional changes. The entire weathering scheme appears to drive the petroleum toward a more even mass-distribution of compounds, which may provide a quantitative and robust biodegradation index.

With regard to specific compounds and compound classes, striking trends in the chemical composition of petroleum are apparent from these studies. During transport from the reservoir to the sea surface, a number of compound classes, representing several hundred distinct compounds, are removed nearly quantitatively. The compound classes most affected include n-alkanes, branched alkanes, isoprenoids, alkyl cyclohexanes, alkyl cyclopentanes, alkyl benzenes, and alkyl napthalenes. The application of physical model incorporating evaporation (gas washing) and dissolution (water washing) indicates that neither of these processes can explain the observed changes in chemical composition – thus indicating these changes are microbial in origin. Biomarkers such as hopanes and steranes in these samples remain unchanged. Differences are also observed between samples at the sea floor and at the sea surface, though not as pronounced as the differences previously discussed. These differences are best explained by evaporation, that is, the low boiling-point compounds are preferentially removed. This may occur through gas washing at the sea floor or through evaporation at the sea surface. While this investigation was geographically limited in scope, focusing on only one seep, the patterns of weathering are striking and provide never-before-seen resolution as to the changes in petroleum composition due to weathering processes.

STUDY PRODUCTS:

One manuscript has been submitted for publication based on this work, and two presentations were recently given. Two additional publications are planned for research resulting in-part from MMS support. These include the results of long-running biodegradation studies and a comparison study of oil composition from various reservoirs offshore reservoirs.

Publications:

American Geophysical Union 2005 Fall Meeting, Wardlaw and Valentine (2005) Petroleum Weathering Associated with Hydrocarbon Migration and Seepage, a Case Study From the Santa Barbara Channel, CA (published abstract).

Wardlaw G, C Reddy, B Nelson, S Arey and D Valentine (submitted to Nature) Biodegradation in the subsurface a selective filter for natural petroleum emissions.

Research Presentations:

American Geophysical Union 2005 Fall Meeting, Valentine, Wardlaw, Kinnaman, Redmond, Kimball, Busso and Larson (2005) Lessons in Microbial Geochemistry from the Coal Oil Point seep field: progess and prospects (published abstract).

FINAL STUDY REPORT

Biodegradation in the subsurface as a selective filter for natural petroleum emissions

George D. Wardlaw[1], Christopher M. Reddy[2], Robert K. Nelson[2], J. Samuel Arey[3] & David L. Valentine[4]

[1]Graduate Program in Marine Science, University of California, Santa Barbara, CA 93106, USA
[2]Woods Hole Oceanographic Institution, Marine Chemistry and Geochemistry Dept, MS#4, Woods Hole, MA 02543 USA
[3]Laboratory of Computational and Biological Chemistry, Swiss Federal Institute of Technology Lausanne, Switzerland
[4]Department of Earth Science and Marine Science Institute, University of California, Santa Barbara, CA 93106 USA

Abstract

Hydrocarbon migration in the deep subsurface is a ubiquitous process in petroleum- and gas-producing regions[1,2]. Hydrocarbons ineffectively trapped by geologic structures gradually migrate to the surface and form areas of intense seepage, with estimated global emissions of 6×10^{11} grams per year into the world's oceans[3]. Subsurface petroleum accumulations with temperatures below ca. 80 ^{o}C are prone to biodegradation, a process leading to the production of heavy oils[4] which are of low economic value and are difficult to extract[5]. Extensive quantification of changes in the chemical composition of biodegraded petroleum has been elusive due to the long timescales involved[6], the heterogeneity of the subsurface and because traditional analyses are unable to resolve or quantify many of the constituent hydrocarbons[7,8]. Here we apply the technique of comprehensive two-dimensional gas chromatography (GC×GC) to quantify differences in the chemical composition of petroleum hydrocarbons sampled from subsurface reservoirs, a proximal seep at the sea floor and the sea surface overlying the seep – all within the Coal Oil Point seep field located offshore Goleta, CA[9]. We show that biodegradation in the subsurface has the greatest impact on hydrocarbon composition with greater than 47% (by mass) loss of petroleum hydrocarbons including systematic changes in the concentration distribution of over 4000 compounds. Evaporation due to gas washing and/or atmospheric exposure is found to be significant once petroleum reaches the sea surface. The quantification of chemical changes described here provides previously unattainable patterns of metabolic preference, and showcases an approach to better quantify the rates and extent of weathering processes for complex hydrocarbon mixtures.

Introduction

The biodegradation of petroleum hydrocarbons is well established for both aerobic[10] and anaerobic prokaryotes[11-13]. The rates and extents of petroleum biodegradation in near-surface environments have been measured directly, but establishing activity in the deep subsurface relies on inferences including variability in the chemical composition of petroleum[1,2,4] and the existence of prokaryotes[14]. Suspected limits on petroleum biodegradation in the subsurface include temperature[2,5], nutrient availability[4], salinity, phase partitioning and the presence of toxins[15]. Degradation patterns of specific biomarkers have previously been compiled and chemical indices have been developed to rank the extent of subsurface petroleum biodegradation[15,16]; still, only a fraction of all petroleum hydrocarbons are typically quantified and little is presently known about the metabolic specificity of anaerobic prokaryotes that consume petroleum in-situ[4].

Most petroleum biodegradation studies typically focus on fewer than a hundred compounds that can be identified and quantified by one-dimensional chromatographic techniques[11,17]. GC×GC provides significant advantages over previous approaches, increasing the number of petroleum hydrocarbons (in the range of C_{10}-C_{43}) that can be resolved and accurately quantified by greater than an order of magnitude[6-8]. This capability is beneficial when analyzing biodegraded petroleum, which typically lacks many of the readily-quantified, and easily degraded, components such as *n*-alkanes[8].

The Coal Oil Point seep field is an established study site located offshore Goleta, CA[3,9]. The seep field is approximately 18 km^2 in area, is located in water depths ranging from 5 to 100 m and is estimated to emit 50 to 170 barrels of oil and 100 to 130 tons of natural gas per day[9]. The geologic structure of the seep field includes a series of crested anticlines formed during folding of the Miocene-age Monterey formation, overlain by more recent deposits[9]. The Monterey Formation is believed to serve as both source rock and geologic trap for local petroleum deposits[9,18]. Oil bearing reservoirs embedded within anticlines are located at depths between 1000 and 1700 m where the ambient temperature ranges between 65-75 ^oC[19]. Oil and gas migrate upward through fractures in the diatomaceous chert of the Monterey Formation[9,18]; these fractures may also provide a conduit for oxidants, nutrients, and possibly prokaryotes to penetrate into the reservoir. Geologic evidence indicates that hydrocarbon seepage occurred in this region for at least the past several hundred thousand years with high temporal and spatial variability[20,21].

The subsurface environment underlying the Coal Oil Point hydrocarbon seeps is presumed anoxic, precluding an important role for aerobic metabolism in the subsurface. Several lines of evidence support this presumption. Gases and production water collected from the reservoirs underlying the seeps contain abundant reduced chemicals such as hydrogen sulphide and ferrous iron[2]. Production waters drawn from the reservoir have been found to harbour populations of strictly-anaerobic prokaryotes including methanogens[14,19]. At the sea floor, seep gas has the odour of hydrogen sulphide, is devoid of oxygen and supports active populations of sulphide-oxidizing bacteria[22] (Supplementary Figure S1). Furthermore, sediments overlying seeps within the COP field have been shown to harbour high rates of sulphate reduction[22]. Given these observations and the limited capacity of seawater to deliver oxygen to the subsurface, it seems likely that sulphate reduction to sulphide and carbon dioxide reduction to methane serve as primary electron accepting processes active in the seep subsurface.

The samples reported here were collected from subsurface oil reservoirs, the sea floor at an active seep, and at the sea surface overlying the seep – all from the COP seep field. Three samples were collected from the oil reservoir, each from active oil wells accessed by Platform Holly. The three wells, 3242-9, 3242-15 and 3242-18 are located at depths of 995 – 1115, 1230 – 1295, and 1025 – 1235 meters respectively, and are at an ambient temperature of 60-70 ^oC. Analysis of the three samples using GC×GC indicates a high degree of similarity, and a sample from well 3242-15 (34°23.370 N by 119° 53.258 W) was chosen for further comparison. Two samples were collected by scuba diver from the sea floor at a location informally known as Jackpot Seep (34°24.175 N by 119°52.670 W, 15 m depth). Both samples were collected as they oozed from the sea floor through an area of exposed bedrock. Two samples were also collected as they reached the sea surface overlying Jackpot Seep; this occurred while the divers collected samples at the sea floor. Chromatographic analysis of the four seep samples indicates a high degree of similarity within the pairs, and one sample from each set was chosen for further comparison. GC×GC chromatograms representative of petroleum from each environment are displayed in Figure 1. In addition, a sample of less-degraded reservoir oil was collected from outside the seep area (Platform Gail; 16-L, 34°07.500 N by 120°24.020 W, 66 ^oC; 1740 m) to serve as a reference.

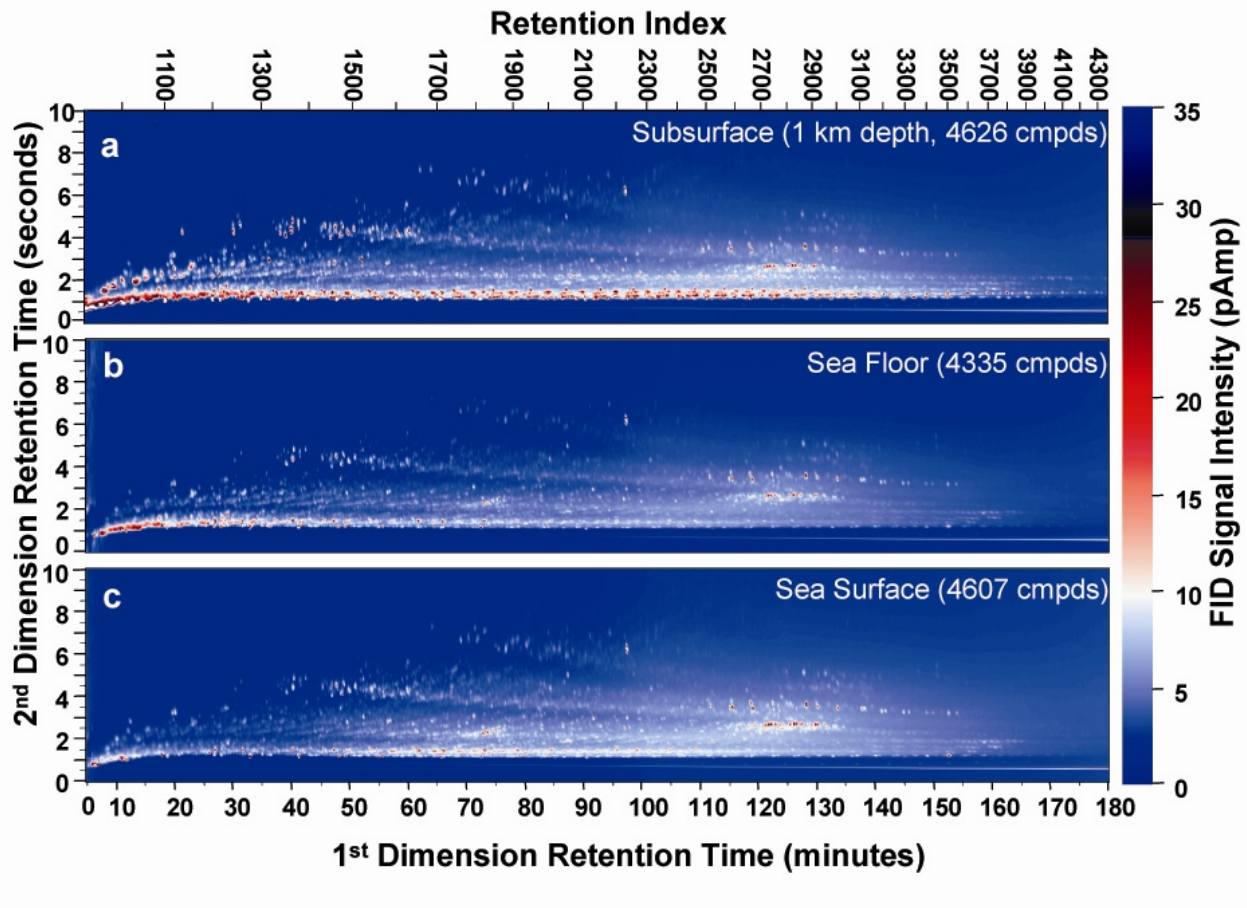

Figure 1. GC×GC with flame ionization detection (FID) chromatograms of (a) crude oil from Platform Holly (Well #2342-15), (b) crude oil collected as it was emerging from the sea floor at Jackpot Seep, and (c) a droplet of crude oil collected as it was spreading on the sea surface above Jackpot Seep. Visual trends represent compound classes as are shown on annotated chromatographs found in Nelson et al. 2006[8]. The C_{30} bacterially-derived biomarker 17α,21β(H)-hopane was used to normalize each image. The retention index employed throughout this manuscript is the Kovats index[29], which is useful for comparing retention between samples analyzed under varying temperature programs or between samples analyzed on different chromatographs.

Application of GC×GC to the chosen samples resulted in the quantification of 4626, 4335, and 4607 distinct hydrocarbon compounds in the reservoir, sea floor and sea surface samples, respectively (Figure 1). The reservoir has been moderately biodegraded in-situ, based on the scale of Wenger et al (2002)[23]. Hopane and sterane biomarkers as well as carbon isotope ratios of bulk oil ($\delta^{13}C$ -23.4 to -22.7 ‰ VPDB) are consistent with petroleum from the Monterey formation[24]. Each sample had similar concentrations of steranes and hopanes, indicating they were likely generated from the same source rock; this was consistent with previous results from the COP field[24]. Numerous compounds quantified in the reservoir samples are absent in the sea floor and sea surface samples (Supplementary Tables S1 and S2), as shown using difference chromatograms (Figure 2)[8]. The disappearance of these compounds in the subsurface is not consistent with evaporation or dissolution processes; rather, it is attributed primarily to the action of anaerobic prokaryotes active in the conduits and reservoirs connecting the source rock to the sea floor.

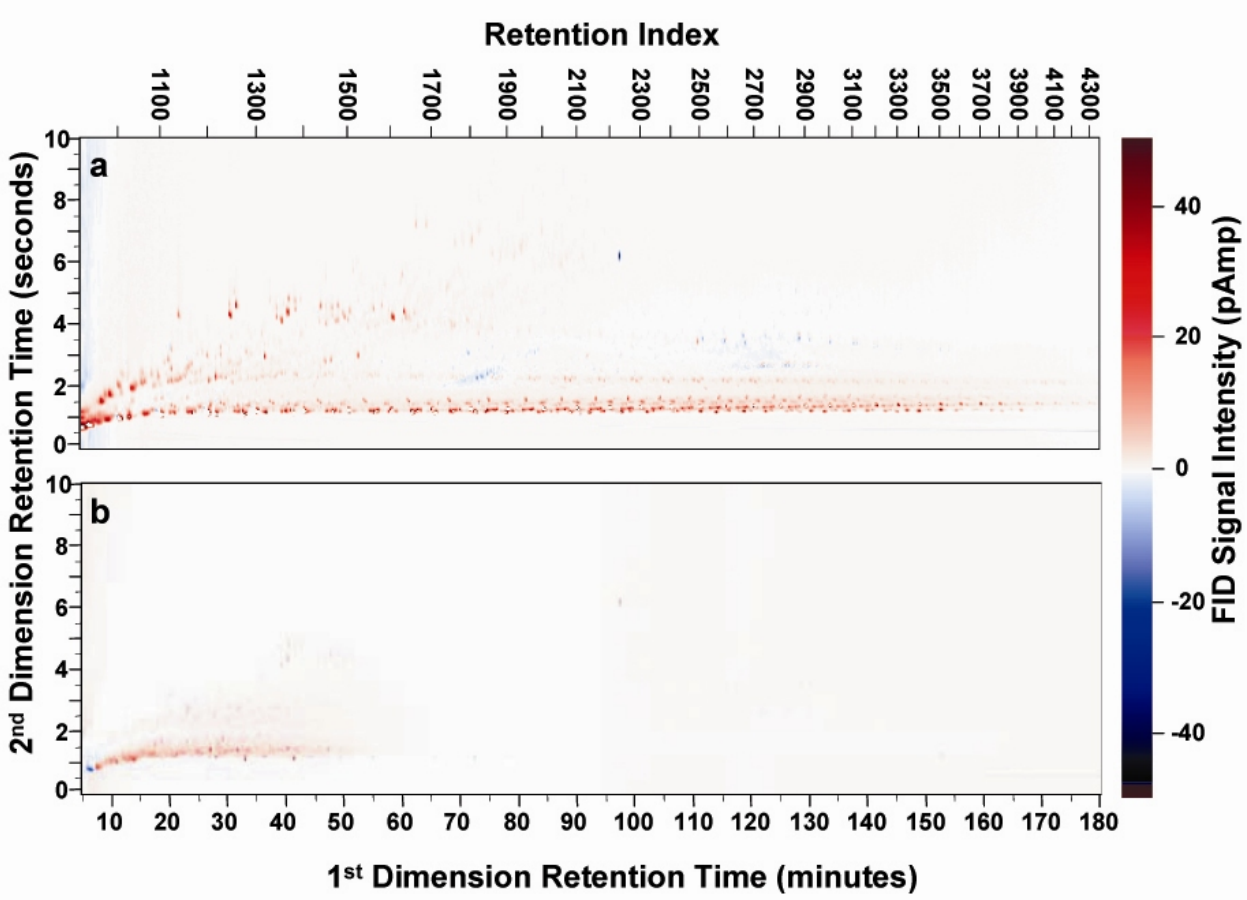

Figure 2. Difference chromatograms produced by (a) subtracting the chromatogram of a sea floor sample (Fig. 1b) from the chromatogram of a reservoir sample (Fig. 1a) and (b) the chromatogram of a sea surface sample (Fig. 1c) from the chromatogram of a sea floor sample (Fig. 1b). The base-plane appears white, while more abundant compounds in (a) the reservoir sample and (b) the sea floor sample appear red. More abundant compounds in (a) the sea floor sample and (b) the sea surface sample appear blue and compounds with little difference in concentration in both samples vanish. These difference chromatograms highlight both the (a) biodegradation of abundant hydrocarbons that occurs in the subsurface as well as (b) the physical processes acting to alter the hydrocarbon composition of the crude oil from the time it reaches the sea floor until its eventual transit to the sea surface. The star shown near the center of the chromatogram denotes the internal standard, dodecadihydrotriphenylene.

Analysis (Figure 3) revealed a trend toward more evenly distributed concentrations of compounds as a result of biodegradation. This trend may prove useful as a quantitative biodegradation index. The compound classes displaying the highest levels of biodegradation between the subsurface and sea floor include many of the components present at high concentration, such as *n*-alkanes, branched/isoprenoid alkanes, alkyl mono-cyclic alkanes, alkyl benzenes, and alkyl naphthalenes (Supplementary Tables S1 and S2). *n*-alkanes and alkyl-benzenes, which respectively represent 10.9% and 8.1% of total petroleum hydrocarbons (TPH) in the reservoir, were quantitatively consumed. Isoprenoids / branched alkanes and alkyl naphthalenes represent 17.5% and 5.2% of TPH in the reservoir and were found to decrease by 85% and 81%, respectively. *n*-alkyl cyclopentanes and *n*-alkyl cyclohexanes together represent 1.5% of TPH, and were found to decrease by 78%. There is an apparent microbial preference for the high molecular weight members of this class (Supplementary Figure S2), with compounds

containing greater than 20 carbons being quantitatively consumed. Concentrations for a subset of over 180 individual compounds are provided in Table S2 of the supplemental on-line information.

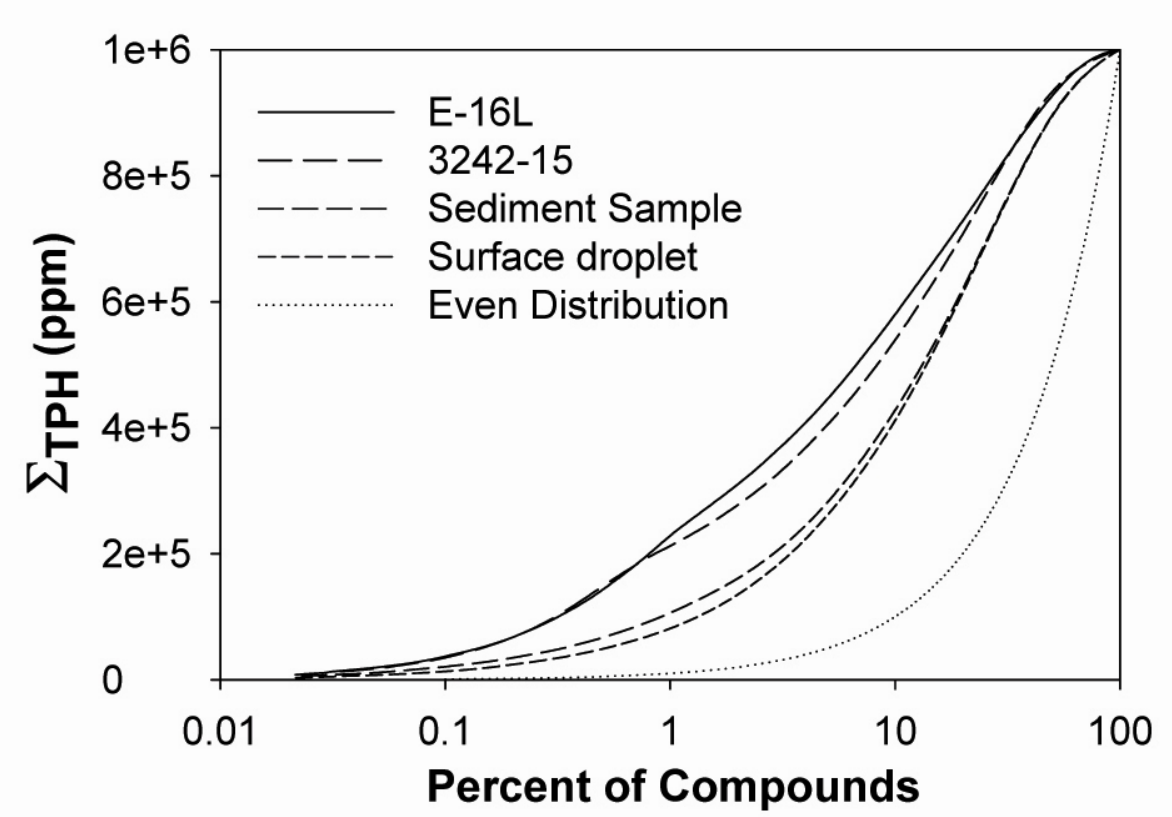

Figure 3. Cumulative rank-distribution for all hydrocarbons quantified in the reservoir, sea floor and sea surface samples. An even distribution of compounds is provided for reference as is a sample of less degraded oil from the Monterey formation. Note the log scale. The number of compounds present in each sample was normalized to 100, and the concentration of each component is provided in ppm, relative to the sum of TPH in the sample.

GC×GC chromatograms allow for elucidation of quantitative signatures indicative of phase transfer to air and water. Patterns of phase transfer are distinguishable because the two-dimensional retention time of each GC×GC peak can be uniquely mapped to the volatility and aqueous solubility of the corresponding hydrocarbon compound[25]. We find no clear evidence for phase transfer in the subsurface, supporting our contention that biodegradation is the responsible mass loss process (Figure 4). Based on duplicate samples collected at the sea floor and the sea surface, we estimate a 10% TPH mass loss due to evaporation during this transition. The mass loss pattern seen in Figure 4 is consistent with evaporation, likely resulting from either gas washing at the sea floor or evaporation at the sea surface. Trends suggest that observed phase transfer rates of ~ C_{12} to C_{15} hydrocarbons are very rapid compared to expected rates based on gas-liquid boundary layer considerations. This suggests that spontaneous spreading at an air-water interface may fractionate volatile compounds based on differences in surface tension among hydrocarbon constituents. No evidence of aqueous dissolution was found, and this

process was not expected to significantly affect TPH composition within the ten to twenty seconds that the oil resided on the sea surface during collection.

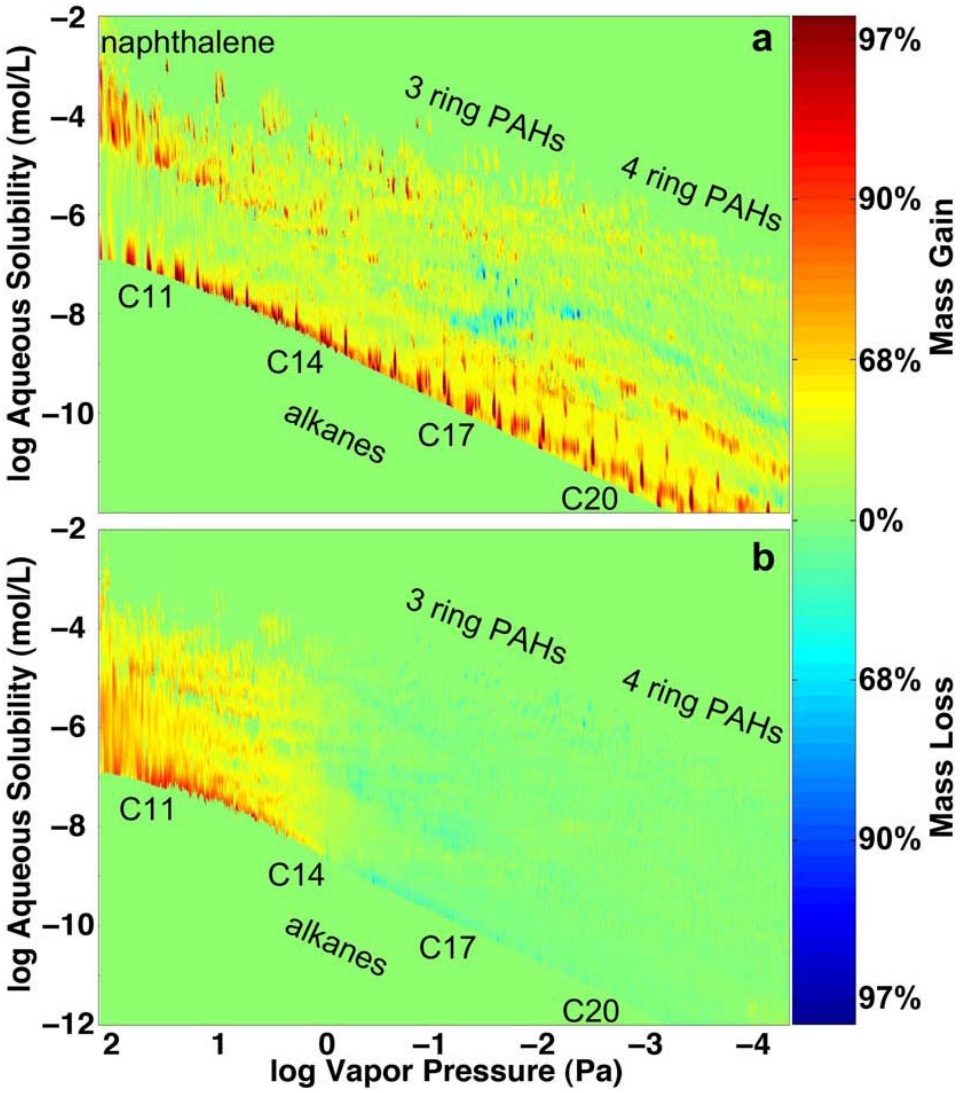

Figure 4. Raw chromatograms were transformed to depict the chromatogram distributed with respect to hydrocarbon log volatility and hydrocarbon log aqueous solubility. Depicted are (a) the log-transformed reservoir sample to sea floor sample ratio and (b) the log-transformed sea floor sample to sea surface sample ratio. Observed trends of mass loss and mass gain (normalized to C_{30} 17α,21β(H)-hopane) suggest that: (a) the sea floor sample is heavily biodegraded with respect to the reservoir sample, rather than evaporated or aqueously dissolved; (b) the sea surface sample is partly evaporated relative to the sea floor sample. Note that the log aqueous solubility assignments are only semi-quantitative estimates below values of about –8 (very sparingly soluble) for the *n*-alkanes series[25]. This did not interfere with any conclusions about water-washing.

This is the first work providing an extensive description of the compounds found in seeping oil and the first to differentiate water washing, evaporation and biodegradation. The ability to identify and quantify thousands of hydrocarbons in a complex mixture such as crude oil represents a significant advance in analytical and environmental chemistry. While many of the compounds resolved here remain unidentified, biodegradation patterns can still be determined

based on retention patterns. Among the as-yet unidentified compounds resolved here, many may serve as biomarkers, providing information about the original source of organic carbon, the environment of deposition, diagenetic processes, the thermal history of the source rock, and the mixing of different oils. For example, we quantified a family of long-chain acyclic and cyclic isoprenoid alkanes, which are presumably derived from archaeal tetra-ethers[26] (Supplemental Table S2). The apparent biodegradation preference for this family is acyclic > dicyclic > tricyclic. Structural characterization of these molecules has the potential to differentiate a depositional source (marine crenarchaea[27]) from a post-depositional source (hyperthermophilic archaea in the subsurface) and to provide other details on the history of the source rock.

The biodegradation filter as described in this work clearly attenuates the emission of numerous hydrocarbons at the COP seep field. While the efficacy of this filter is dependent on factors such as the geologic setting and petroleum flux rate, it is apparent from the widespread distribution of biodegraded oils that this filter is globally important. Approximately 6×10^{11} grams of crude oil per year is estimated to seep from the subsurface to the sea surface[3, 28]. Assuming that rates of crude oil seepage in terrestrial settings are similar in magnitude and that a 50% loss of hydrocarbons is typical, we estimate that greater than 10^{12} grams per year of hydrocarbons are likely degraded prior to the escape of residual crude oil. This is equivalent to an annual economic loss of greater than half a billion US dollars. Significantly more than this amount is likely biodegraded to such an extent that it becomes trapped permanently in the subsurface. Athabasca and Orinoco oil fields, the two largest in the world, are examples of such biodegraded accumulations.

References Cited

1. Aitken, C. M., Jones, D. M., & Larter, S. R. Anaerobic hydrocarbon biodegradation in deep subsurface oil reservoirs. *Nature* **431**, 291-294 (2004).

2. Willhelms, A. *et al.* Biodegradation of oil in uplifted basins prevented by deep-burial sterilization. *Nature* **411**, 1034-1037 (2001).

3. Kvenvolden, K. A. & Cooper, C. K. Natural seepage of crude oil into the marine environment. *Geo.-Marr. Lett.*, **23,** 140-146 (2003).

4. Head, I. M., Jones, D. M., & Larter, S. R. Biological activity in the deep subsurface and the origin of heavy oil. *Nature,* **426**, 344-352 (2003).

5. Connan, J. in *Advances in Petroleum Geochemistry* Vol. 1 (eds Brooks, J & Welte, D. H.) 299-335 Academic Press, London (1984).

6. Reddy, C. M. *et al.* The West Falmouth oil spill after thirty years: the persistence of petroleum hydrocarbons in marsh sediments. *Environ. Sci. Technol.* **36,** 4754-4760 (2002).

7. Frysinger, G. S., Gaines, R. B., Xu, L., & Reddy, C. M. Resolving the unresolved complex mixture in petroleum-contaminated sediments. *Environ. Sci. Technol.* **37**, 1653-1662 (2003).

8. Nelson, R. K. *et al.* Tracking the weathering of an oil spill with comprehensive two-dimensional gas chromatography. *Environ. Forensics* **7,** 1-12 (2006).

9. Hornafius, J. S., Quigley D., & Luyendyk, B. P. The world's most spectacular marine hydrocarbon seeps (Coal Oil Point, Santa Barbara Channel, California): quantification of emissions. *J. Geophys. Res.-Oceans* **104**, 20703-20711 (1999).

10. Atlas, R. M., & Bartha R. Hydrocarbon biodegradation and oil-spill bioremediation. *Adv. Microb. Ecol.* **12**, 287-338 (1992).

11. Spormann, A. M. & Widdel, F. Metabolism of alkylbenzenes, alkanes, and other hydrocarbons in anaerobic bacteria. *Biodegradation* **11,** 85-105 (2000).

12. Coates, J. D., Woodward, J., Allen, J., Philp, P., & Lovley, D. R. Anaerobic degradation of polycyclic aromatic hydrocarbons and alkanes in petroleum-contaminated marine harbour sediments. *Appl. Environ. Microbiol.* **63,** 3589-3593 (1997).

13. Rueter, P. *et al.* Anaerobic oxidation of hydrocarbons in crude-oil by new types of sulfate-reducing bacteria. *Nature* **372,** 455-458 (1994).

14. Orphan, V. J., Boles, J., Goffredi, S. K. & DeLong, E. F. Geochemical influence on community structure and microbial processes in high temperature oil reservoirs. *Geomicrobiol. J.* **20,** 295-311 (2003).

15. Peters, K. K., Walters, C. C. & Moldowan, J. M. in *The Biomarker Guide, Biomarkers and Isotopes in Petroleum Exploration and Earth History*. 2nd Edition. II 646-650, Cambridge University Press, Cambridge, MA (2002).

16. Peters, K. K., Walters, C. C. & Moldowan, J. M. in *The Biomarker Guide, Biomarkers and Isotopes in the Environment and Human History*. 2nd Edition I 198-251, Cambridge University Press, Cambridge, MA (2002).

17. Van Hamme, J. D., Singh, A., & Ward, O. P. Recent advances in petroleum microbiology. *Microbiol. Mol. Biol. Rev* **67,** 503-549 (2003)

18. Reed, W. E. & Kaplan, I. R. The chemistry of marine petroleum seeps. *J. Geochem. Explor.* **7**, 255-293 (1977).

19. Orphan, V. J., Taylor, L. T. Hafenbradl, D., & DeLong, E. F. Culture-dependent and culture-independent characterization of microbial assemblages associated with high-temperature petroleum reservoirs. *Appl. Environ. Microbiol.* **66,** 700-711 (2000).

20. Boles, J. R., Eichhubl, P**.**, Garven, G., & Chen, J. Evolution of a hydrocarbon migration pathway along basin-bounding faults: evidence from fault cement. *AAPG Bull*. **88**, 947-970 (2004).

21. Hill, T.M. *et al.* Late Quaternary evidence for climatically driven hydrocarbon emissions. (in revision at PNAS) (2006).

22. Bauer, J.E., Montagna, P.A. Spies, R.B. Hardin, D.D. & Prieto M. Microbial biogeochemistry and heterotrophy in sediments of a marine hydrocarbon seep. *Limnol. Oceanogr.* **33**, 1493-1513 (1988).

23. Wenger, L. M., Davis, C. L., & Isaksen, G. H. *Multiple Controls on Petroleum Biodegradation and Impact in Oil Quality*. (SPE71450, Society of Petroleum Engineers, 2001).

24. Hostettler, F. D., Rosenbauer, R. J., Lorenson, T. D., & Dougherty, J. Geochemical characterization of tarballs on beaches along the California coast. Part I - shallow seepage impacting the Santa Barbara Channel Islands, Santa Cruz, Santa Rosa and San Miguel. *Org. Geochem.* **35,** 725-746 (2004).

25. Arey, S. J., Nelson, R. K., Xu, L., & Reddy, C. M. Using comprehensive two-dimensional gas chromatography retention indices to estimate environmental partitioning properties for a complete set of diesel fuel hydrocarbons. *Anal. Chem.* **77**, 7172-7182 (2005).

26. Ventura, G. T. Biomarkers of hydrothermally altered, late Archean metasediments from the southern Abitibi subprovince of Ontario, Canada. PhD thesis, Department of Earth and Environmental Sciences, University of Illinois at Chicago, (July, 2006).

27. DeLong, E. F. *et al.* Dibiphytanyl ether lipids in nonthermophilic crenarchaeotes. *Appl. Environ. Microbiol.* **64**, 1133-1138 (1998).

28. National Research Council *Oil in the Sea: Inputs, Fates and Effects*. Washington, D.C.: National Academy Press, May. NRC (2003).

29. Kovats, E. Gas chromatographic characterization of organic substances in the retention index system. *Advan. Chromatog*. 1:229-247 (1965).

Acknowledgements

We thank S. Horner and Venoco Inc. for providing access to reservoir samples. We also thank J. Boles for providing advice on the geologic structure of the COP field. We acknowledge support from the US Minerals Management Service (Task 85338 to DLV), the US National Science Foundation (OCE-0447395 to DLV and IIS-0430835 to CMR), the California Toxic Substance Research and Training Program (19909 to GDW), and the US Department of Energy (DE-FG02-06ER15775 to CMR).

Supplementary Methods

The hydrocarbon composition of three oil samples collected at the sea surface, on the sea floor, and from a production well on Platform Holly were analyzed as the hexane soluble extracts of each sample by comprehensive two-dimensional gas chromatography (GC×GC), which can separate an order of magnitude more petroleum hydrocarbons than traditional gas chromatography (Frysinger et al., 2003; Figure 1). For a more detailed discussion on this technology, refer to Reddy et al. (2002). Briefly, the oil samples were dissolved in hexane at a concentration of 4 mg/mL, sodium sulphate was added to remove any traces of water. The samples were mixed vigorously on a vortex mixer and then allowed to stand overnight. The soluble hydrocarbon fraction was decanted into a clean vial and the insoluble material which precipitated out of solution (asphaltenes) was discarded.

Supplementary Figure S1. An image of oil seeping from the sea floor at Jackpot Seep. The white thread-like filaments shown here are composed of uncharacterized sulphide-oxidizing bacteria. Scale bar = 1 cm.

Separation of petroleum hydrocarbons was achieved with a GC×GC system employing an Agilent 6890 gas chromatograph configured with a 7683 series split/splitless auto-injector, two capillary gas chromatography columns, a model KT-CLM-ZOE02 loop jet modulator (Zoex Corporation, Lincoln, NE), and a flame ionization detector. Each reservoir sample was injected in splitless mode and the purge vent was opened at 2.5 minutes. The inlet temperature was 300°C. The first-dimension column and the loop jet modulator reside in the main oven of the Agilent 6890 gas chromatograph. The second-dimension column is housed in a smaller oven

installed on the right side of the main oven. With this configuration, the temperature profiles of the first-dimension column, thermal modulator (hot jet), and the second-dimension column can be independently programmed. The first-dimension column was a nonpolar 100% dimethyl polysiloxane phase (Restek Rtx-1 Crossbond, 6.5m length, 0.10mm I.D., 0.4 μm film thickness) that was programmed to remain isothermal at 37°C for 5 minutes and then ramped from 37 to 307° C at 1.5°C min^{-1}. The modulation loop was deactivated fused silica (1.6m length, 0.10mm I.D.). The thermal modulator (hot jet) was heated to 100°C above the temperature in the main oven to insure that all trapped compounds were thoroughly and rapidly desorbed from the cold spot. Second-dimension separations were performed on a 50% phenyl polysilphenylene-siloxane column (SGE BPX50, 0.8m length, 0.10mm I.D., 0.1 μm film thickness) that was programmed to remain isothermal at 70°C for 5 minutes and then ramped from 70 to 340°C at 1.5°C min^{-1}. The thermal modulator loop pulse frequency was 10 seconds (0.10 Hz), and the pulse width was 300 milliseconds. The cold jet gas was dry N_2 chilled with liquid Argon at a flow rate of 4.0 L min^{-1}. The carrier gas was H_2 at a constant flow rate of 1.5 mL min^{-1}. The FID signal was sampled at 100 Hz. Peaks were identified with commercially available standards from Aldrich Chemical, National Institute of Standards and Technology (NIST), and Chiron. Dodecadihydrotriphenylene was used as an internal standard and eluted at 92.4 minutes on the x-axis and at 5.7 seconds on the y-axis (Figure 1 and Figure 2).

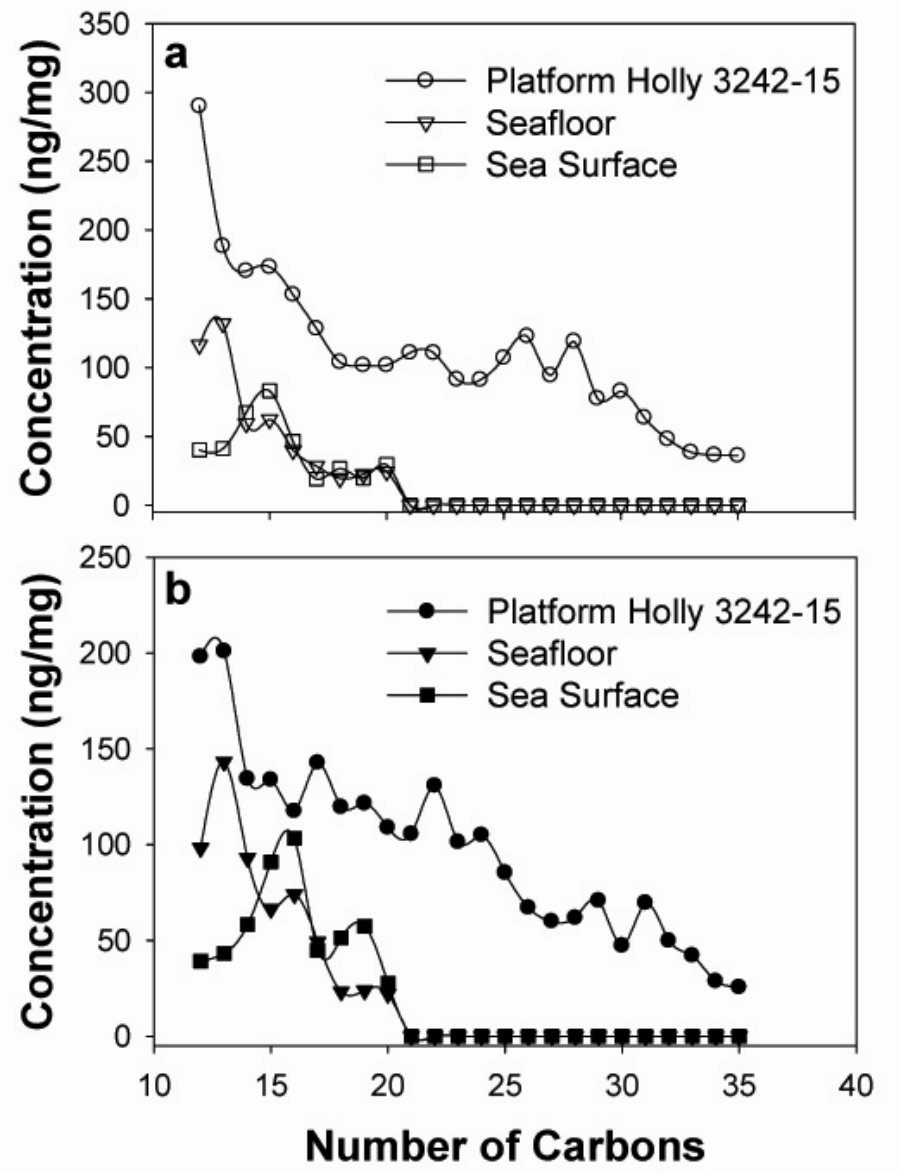

Supplemental Figure S2. A graph of (a) *n*-alkyl cyclopentanes and (b) *n*-alkyl cyclohexanes containing various numbers of carbons, versus concentration. The pattern of compound loss between the reservoir and sea floor, particularly for compounds greater than 20 carbons in size, indicates a preference for these compounds by *in-situ* microbes. The preferential loss of low-carbon-number compounds between the sea floor and sea surface is attributed to evaporation.

The GC×GC FID data was processed with GC Image software (GC Image, LLC, Lincoln NE; Reichenbach *et al*., 2003; 2004). Each GC×GC image was base-plane subtracted to remove the FID offset (Reichenbach *et al.,* 2003). Peak volumes of the resolved components in each of the GC×GC images were measured with the GC Image software. In order to set the threshold peak detection values in the GC Image software, the data in each GC×GC chromatogram was visually inspected in tabular form (spreadsheet) as well as in colour contour plots (plan view) and three dimensional surface rendering (mountain plots) formats. The peak detection filter was set to exclude all peaks which where one-half the volume or less than the smallest peak detected

visually in any of the chromatograms. Using these settings, we detected between 4,000 and 5,000 components in each chromatogram. Peaks representing less than 0.02 ng of material did not meet our peak detection criteria and were excluded from our analysis.

Supplementary Table S1. Concentrations of major hydrocarbon classes.

	Reservoir (µg/mg)*	Sea floor (µg/mg)*	Sea Surface (µg/mg)*
Total petroleum hydrocarbons	338	181	203
alkanes	164	59.6	52.8
branched and isoprenoid alkanes	59.0	9.20	11.0
normal alkanes	36.8	0.00	0.00
n-alkyl cyclohexanes	2.30	0.60	0.50
n-alkyl cyclopentanes	2.60	0.50	0.40
alkyl benzenes	27.4	0.00	0.00
naphthalenes	17.7	13.9	20.7
phenanthrenes	7.90	10.1	6.70

*Concentration is in micrograms compound per mg of oil analyzed.

Appendix 1

Compound	Reservoir[a] (ng/mg)	Sea floor[b] (ng/mg)	Sea-Surface[c] (ng/mg)	% loss Reservoir to Sflr	% loss Reservoir to Ssrf
C_{12} *n*-alkyl cyclohexane	198	98.3	39.2	50.4	80.2
C_{13} *n*-alkyl cyclohexane	201	143	43.3	28.7	78.4
C_{14} *n*-alkyl cyclohexane	135	93.0	58.3	30.8	56.7
C_{15} *n*-alkyl cyclohexane	134	66.4	90.9	50.4	32.0
C_{16} *n*-alkyl cyclohexane	118	74.1	104	37.0	12.0
C_{17} *n*-alkyl cyclohexane	143	49.3	44.8	65.4	68.6
C_{18} *n*-alkyl cyclohexane	120	23.3	51.4	80.5	57.1
C_{19} *n*-alkyl cyclohexane	122	23.8	57.5	80.4	52.7
C_{20} *n*-alkyl cyclohexane	109	22.1	27.7	79.7	74.6
C_{21} *n*-alkyl cyclohexane	106	0	0	100	100
C_{22} *n*-alkyl cyclohexane	131	0	0	100	100
C_{23} *n*-alkyl cyclohexane	101	0	0	100	100
C_{24} *n*-alkyl cyclohexane	105	0	0	100	100
C_{25} *n*-alkyl cyclohexane	85.3	0	0	100	100
C_{26} *n*-alkyl cyclohexane	67.0	0	0	100	100
C_{27} *n*-alkyl cyclohexane	60.0	0	0	100	100
C_{28} *n*-alkyl cyclohexane	61.8	0	0	100	100
C_{29} *n*-alkyl cyclohexane	70.8	0	0	100	100
C_{30} *n*-alkyl cyclohexane	47.3	0	0	100	100
C_{31} *n*-alkyl cyclohexane	69.5	0	0	100	100
C_{32} *n*-alkyl cyclohexane	49.8	0	0	100	100
C_{33} *n*-alkyl cyclohexane	42.1	0	0	100	100
C_{34} *n*-alkyl cyclohexane	28.7	0	0	100	100
C_{35} *n*-alkyl cyclohexane	25.6	0	0	100	100
C_{12} *n*-alkyl cyclopentane	291	117	40.2	59.8	86.1
C_{13} *n*-alkyl cyclopentane	189	132	41.3	29.8	78.1

C_{14} *n*-alkyl cyclopentane	170	59.5	67.5	65.1	60.3
C_{15} *n*-alkyl cyclopentane	173	62.4	83.2	64.0	52.0
C_{16} *n*-alkyl cyclopentane	153	40.0	46.4	73.8	69.7
C_{17} *n*-alkyl cyclopentane	128	28.5	19.2	77.8	85.1
C_{18} *n*-alkyl cyclopentane	104	19.6	26.8	81.1	74.3
C_{19} *n*-alkyl cyclopentane	102	22.6	19.8	77.8	80.5
C_{20} *n*-alkyl cyclopentane	102	24.5	29.5	75.9	71.0
C_{21} *n*-alkyl cyclopentane	111	0	0	100	100
C_{22} *n*-alkyl cyclopentane	111	0	0	100	100
C_{23} *n*-alkyl cyclopentane	91.4	0	0	100	100
C_{24} *n*-alkyl cyclopentane	91.2	0	0	100	100
C_{25} *n*-alkyl cyclopentane	107	0	0	100	100
C_{26} *n*-alkyl cyclopentane	123	0	0	100	100
C_{27} *n*-alkyl cyclopentane	94.4	0	0	100	100
C_{28} *n*-alkyl cyclopentane	119	0	0	100	100
C_{29} *n*-alkyl cyclopentane	77.6	0	0	100	100
C_{30} *n*-alkyl cyclopentane	82.9	0	0	100	100
C_{31} *n*-alkyl cyclopentane	63.7	0	0	100	100
C_{32} *n*-alkyl cyclopentane	48.1	0	0	100	100
C_{33} *n*-alkyl cyclopentane	38.6	0	0	100	100
C_{34} *n*-alkyl cyclopentane	36.6	0	0	100	100
C_{35} *n*-alkyl cyclopentane	36.1	0	0	100	100
ααα(S)C27 cholestane	189	114	145	39.8	23.3
αββ(R)C27 cholestane	203	185	200	9.2	1.5
αββ(S)C27 cholestane	192	181	215	5.8	-12.0
ααα(R)C27 cholestane	233	162	193	30.5	17.2
ααα (S) C28 ergostane	166	126	140	24.0	15.6
αββ(R)C28 ergostane	269	174	245	35.4	8.9
αββ(S)C28 ergostane	180	175	175	3.0	3.1
ααα(R)C28 ergostane	215	141	196	34.4	8.7

ααα(S)C29 stigmastane	157	101	133	36.1	15.3
αββ(R)C29 stigmastane	230	134	195	41.7	15.2
αββ(S)C29 stigmastane	134	115	132	14.7	1.8
ααα(R)C29 stigmastane	153	134	159	12.5	-3.9
28,30-bisnorhopane	360	409	403	-13.4	-11.9
norhopane	223	288	164	-29.2	26.5
C_{30} hopane	214	183	221	14.3	-3.4
31S homohopane	138	131	123	5.1	10.6
31R homohopane	116	97.8	101	15.4	12.3
32S homohopane	129	142	107	-10.3	16.9
32R homohopane	91.8	117	90.5	-27.4	1.3
33S homohopane	93.7	126	107	-34.3	-13.6
33R homohopane	108	92.0	91.4	14.5	15.0
34S homohopane	99.3	91.8	63.1	7.5	36.5
34R homohopane	93.0	68.5	51.6	26.4	44.6
35S homohopane	119	143	102	-20.0	14.2
35R homohopane	81.5	93.8	71.1	-15.1	12.7
gammacerane	70.7	53.6	47.6	24.2	32.6
farnesane	1.41x10^3	159	165	88.8	88.3
norpristane	1.57x10^3	111	133	93.0	91.6
pristane	1.71x10^3	84.5	116	95.0	93.2
phytane	2.19x10^3	130	227	94.1	89.7
cyclic isoprenoid alkane 01	257	48.5	65.0	81.1	74.7
cyclic isoprenoid alkane 02	190	41.1	68.7	78.3	63.7
cyclic isoprenoid alkane 03	93.6	35.3	32.7	62.2	65.1
cyclic isoprenoid alkane 04	114	18.6	24.7	83.6	78.3
cyclic isoprenoid alkane 05	217	23.4	25.2	89.2	88.4
cyclic isoprenoid alkane 06	288	41.4	56.8	85.6	80.3
cyclic isoprenoid alkane 07	371	85.5	116	77.0	68.8

(biphytane)					
cyclic isoprenoid alkane 08	108	22.7	32.4	79.0	69.9
monocyclic isoprenoidal alkane 01	-	46.1	47.9	-	
monocyclic isoprenoidal alkane 02	-	29.3	41.1	-	
monocyclic isoprenoidal alkane 03	-	42.2	49.4	-	
monocyclic isoprenoidal alkane 04	-	34.7	40.6	-	
dicyclic isoprenoidal alkane 01	42.2	34.2	44.1	18.9	-4.6
dicyclic isoprenoidal alkane 02	53.1	35.8	61.2	32.5	-15.3
dicyclic isoprenoidal alkane 03	55.9	39.2	48.7	29.9	12.8
dicyclic isoprenoidal alkane 04	57.4	27.0	30.0	53.0	47.6
dicyclic isoprenoidal alkane 05	69.6	28.4	62.1	59.2	10.9
dicyclic isoprenoidal alkane 06	117	45.2	66.7	61.3	42.9
dicyclic isoprenoidal alkane 07	33.2	24.7	34.8	25.7	-4.8
tricyclic isoprenoidal alkane 01	47.2	40.7	62.1	13.7	-31.7
tricyclic isoprenoidal alkane 02	65.0	59.0	67.3	9.2	-3.5
tricyclic isoprenoidal alkane 03	53.4	44.9	61.9	16.0	-15.9
tricyclic isoprenoidal alkane 04	47.3	41.1	45.5	13.0	3.6
tricyclic isoprenoidal alkane 05	38.0	20.6	26.8	45.8	29.3
tricyclic isoprenoidal alkane 06	74.5	50.3	65.7	32.6	11.8
tricyclic isoprenoidal alkane 07	36.0	23.7	39.5	34.1	-9.7
tricyclic isoprenoidal alkane 08	63.3	40.5	66.1	36.1	-4.4
tricyclic isoprenoidal alkane 09	55.6	42.9	52.4	22.8	5.7
tricyclic isoprenoidal alkane 10	45.4	39.0	48.5	14.0	-7.0
tricyclic isoprenoidal alkane 11	49.6	40.8	52.5	17.8	-5.8
tricyclic isoprenoidal alkane 12	34.5	33.9	42.3	1.6	-22.6
n-C_{10}	1.73x10^3	0	0	100	100

n-C_{11}	1.78x10^3	0	0	100	100
n-C_{12}	1.86x10^3	0	0	100	100
n-C_{13}	2.05x10^3	0	0	100	100
n-C_{14}	2.18x10^3	0	0	100	100
n-C_{15}	2.32x10^3	0	0	100	100
n-C_{16}	2.24x10^3	0	0	100	100
n-C_{17}	2.12x10^3	0	0	100	100
n-C_{18}	2.22x10^3	0	0	100	100
n-C_{19}	1.94x10^3	0	0	100	100
n-C_{20}	2.07x10^3	0	0	100	100
n-C_{21}	1.81x10^3	0	0	100	100
n-C_{22}	1.83x10^3	0	0	100	100
n-C_{23}	1.58x10^3	0	0	100	100
n-C_{24}	1.51x10^3	0	0	100	100
n-C_{25}	1.13x10^3	0	0	100	100
n-C_{26}	1.01x10^3	0	0	100	100
n-C_{27}	879	0	0	100	100
n-C_{28}	742	0	0	100	100
n-C_{29}	652	0	0	100	100
n-C_{30}	594	0	0	100	100
n-C_{31}	519	0	0	100	100
n-C_{32}	415	0	0	100	100
n-C_{33}	321	0	0	100	100
n-C_{34}	261	0	0	100	100
n-C_{35}	216	0	0	100	100
n-C_{36}	197	0	0	100	100
n-C_{37}	201	0	0	100	100
n-C_{38}	173	0	0	100	100
n-C_{39}	75.8	0	0	100	100

n-C_{40}	60.1	0	0	100	100
n-C_{41}	34.3	0	0	100	100
n-C_{42}	35.7	0	0	100	100
n-C_{43}	32.2	0	0	100	100
indan	386	104	71.8	73.2	81.4
tetralin	148	104	119	29.8	19.6
C_{14} linear alkyl benzene	28.5	0	0	100	100
C_{15} linear alkyl benzene	33.3	0	0	100	100
C_{16} linear alkyl benzene	50.3	0	0	100	100
C_{17} linear alkyl benzene	52.4	0	0	100	100
C_{18} linear alkyl benzene	65.4	0	0	100	100
C_{19} linear alkyl benzene	75.9	0	0	100	100
C_{20} linear alkyl benzene	93.8	0	0	100	100
C_{21} linear alkyl benzene	79.9	0	0	100	100
C_{22} linear alkyl benzene	84.1	0	0	100	100
C_{23} linear alkyl benzene	78.5	0	0	100	100
C_{24} linear alkyl benzene	92.2	0	0	100	100
C_{25} linear alkyl benzene	85.7	0	0	100	100
C_{26} linear alkyl benzene	100	0	0	100	100
C_{27} linear alkyl benzene	53.6	0	0	100	100
C_{28} linear alkyl benzene	58.8	0	0	100	100
C_{29} linear alkyl benzene	61.2	0	0	100	100
C_{30} linear alkyl benzene	65.6	0	0	100	100
C_{31} linear alkyl benzene	41.4	0	0	100	100
C_{32} linear alkyl benzene	28.9	0	0	100	100
C_{33} linear alkyl benzene	33.1	0	0	100	100
C_{34} linear alkyl benzene	26.6	0	0	100	100
C_{35} linear alkyl benzene	20.7	0	0	100	100

C_{36} linear alkyl benzene	21.9	0	0	100	100
C_{37} linear alkyl benzene	17.0	0	0	100	100
C_{38} linear alkyl benzene	12.7	0	0	100	100
C_{39} linear alkyl benzene	20.4	0	0	100	100
C_{40} linear alkyl benzene	23.2	0	0	100	100
naphthalene	179	4.4	4.2	97.5	97.7
2-methylnaphthalene	460	45.9	28.3	90.0	93.9
1-methylnaphthalene	300	26.6	15.7	91.1	94.8
biphenyl	24.6	3.5		85.8	100.0
1-ethylnaphthalene	76.3	21.3	14.3	72.0	81.3
2,6-dimethylnapthalene	354	96.4		72.8	82.7
acenaphthene	10.1	7.0	4.6	30.8	54.0
fluorene	101	27.7	61.4	72.5	65.9
phenanthrene	66.5	25.6	31.5	61.5	52.6
1-methylphenanthrene	51.7	25.9	23.4	49.8	54.7
[d]dodecadyhydrotriphenylene	629	623	617		

[a] Reservoir sample from Platform Holly Well 3242-15.
[b] Sediment surface sample from Jackpot seep.
[c] Sea surface sample collected overlying Jackpot see.
d. Dodecadihydrotriphenylene was used as the internal standard.

Supplemental References

1. Reddy, C. M. *et al.* The West Falmouth oil spill after thirty years: the persistence of petroleum hydrocarbons in marsh sediments. *Environ. Sci. Technol.* **36,** 4754-4760 (2002).

2. Frysinger, G. S., Gaines, R. B., Xu, L., & Reddy, C. M., Resolving the unresolved complex mixture in petroleum-contaminated sediments. *Environ. Sci. Technol.* **37**, 1653-1662 (2003).

3. Reichenbach, S. E., Ni, M. T., Kottapalli, V., & Visvanathan, A. Information technologies for comprehensive two-dimensional gas chromatography. *Chemom. Intell. Lab. Syst.* **71**, 107-120 (2004).

4. Reichenbach, S. E., Ni, M. T., Zhang, D. M., & Ledford E. B., Image background removal in comprehensive two-dimensional gas chromatography. *J. Chromatogr. A* **985**: 47-56 (2005).

The Department of the Interior Mission

As the Nation's principal conservation agency, the Department of the Interior has responsibility for most of our nationally owned public lands and natural resources. This includes fostering sound use of our land and water resources; protecting our fish, wildlife, and biological diversity; preserving the environmental and cultural values of our national parks and historical places; and providing for the enjoyment of life through outdoor recreation. The Department assesses our energy and mineral resources and works to ensure that their development is in the best interests of all our people by encouraging stewardship and citizen participation in their care. The Department also has a major responsibility for American Indian reservation communities and for people who live in island territories under U.S. administration.

The Minerals Management Service Mission

As a bureau of the Department of the Interior, the Minerals Management Service's (MMS) primary responsibilities are to manage the mineral resources located on the Nation's Outer Continental Shelf (OCS), collect revenue from the Federal OCS and onshore Federal and Indian lands, and distribute those revenues.

Moreover, in working to meet its responsibilities, the **Offshore Minerals Management Program** administers the OCS competitive leasing program and oversees the safe and environmentally sound exploration and production of our Nation's offshore natural gas, oil and other mineral resources. The MMS **Royalty Management Program** meets its responsibilities by ensuring the efficient, timely and accurate collection and disbursement of revenue from mineral leasing and production due to Indian tribes and allottees, States and the U.S. Treasury.

The MMS strives to fulfill its responsibilities through the general guiding principles of: (1) being responsive to the public's concerns and interests by maintaining a dialogue with all potentially affected parties and (2) carrying out its programs with an emphasis on working to enhance the quality of life for all Americans by lending MMS assistance and expertise to economic development and environmental protection.